Formation and evolution of a self-organized hierarchy of Ge nanostructures on Si(111)-(7×7): STM observations and first-principles calculations

H. F. Ma, Z. H. Qin, M. C. Xu, D. X. Shi, and H.-J. Gao*
Institute of Physics, Chinese Academy of Sciences, Beijing 100080, China

Sanwu Wang†
Department of Physics and Engineering Physics, University of Tulsa, Tulsa, Oklahoma 74104, USA

Sokrates T. Pantelides‡
Department of Physics and Astronomy, Vanderbilt University, Nashville, Tennessee 37235, USA
and Materials Sciences and Technology Division, Oak Ridge National Laboratory, Oak Ridge, Tennessee 37831, USA
(Received 30 October 2006; revised manuscript received 29 January 2007; published 5 April 2007)

We report scanning-tunneling-microscopy observations and first-principles calculations for the formation and evolution of self-organized Ge nanostructures on Si(111)-(7×7) surfaces for Ge coverages up to 0.5 ML. We show that individual Ge atoms initially form a triangular lattice. At higher coverages, Ge nanoparticles 1 nm in diameter gradually form in both the faulted and unfaulted half unit cells with an initial preference in the faulted halves, ultimately driving ordered hexagonal arrays. The underlying 7×7 surface periodicity, the triangular single-Ge lattice, and the nanoparticle hexagonal superstructures coexist. Charge transfer from Si adatoms to Ge nanoparticles is shown to play a key role in the self-organization.

DOI: 10.1103/PhysRevB.75.165403 PACS number(s): 68.43.−h, 68.47.Fg, 73.22.−f, 81.16.Rf

I. INTRODUCTION

Germanium-based nanostructures grown on silicon substrates have been studied extensively in recent years due to their potential applications in optoelectronics and nanotechnology.[1–5] While Ge nanostructures have so far been mostly investigated on Si(100) surfaces,[2–5] there has been increasing interest in the formation of Ge nanostructures on the Si(111) surface,[6–15] especially the 7×7 reconstruction whose rich structure offers a wide range of possibilities. Indeed, several groups have reported formation of distinct types of Ge nanostructures.[6–15] In particular, ordered hexagonal Ge nanostructures were obtained on Si(111)-(7×7) at a Ge coverage of 0.5 ML by Ansari *et al.*[13] The existence of such diverse nanostructures raises questions about the evolution of self-assembly as a function of coverage, which is a key factor in achieving control and implementing directed self-assembly.

In this paper, we report systematic scanning-tunneling-microscopy (STM) observations of the growth and evolution of Ge nanostructures on Si(111)-(7×7) surfaces at coverages up to 0.5 ML and with the temperature of the substrate kept at 150 °C, complemented by first-principles quantum-mechanical calculations.

The remainder of this paper is organized as follows. In Sec. II, we provide a description of the experimental and theoretical methods that we used. In Sec. III, we present and discuss our STM observations and theoretical results. In Sec. IV, we summarize the main conclusions obtained from our STM measurements and theoretical investigations based on first-principles density-functional calculations.

II. EXPERIMENTAL AND THEORETICAL METHODS

The experiments were carried out in an ultrahigh-vacuum (UHV) chamber with a base pressure below 6×10^{-11} mbar. All substrates used in this work were cut from a commercial lightly phosphorus-doped *n*-type Si(111) wafers (orientation $<0.5°$) with a resistivity of 7.5 Ω cm and a thickness of 0.381 mm. The substrate was cleaned through a strict process before it was inserted in the UHV chamber via a load-lock chamber. The cleaning process involved several rinsing cycles for the sample in reagent-grade ethanol and subsequently in de-ionized water. After cleaning, the Si sample was mounted on a Mo stage using ceramic tweezers, and four Ta strips were used to fix the sample. The substrate was degassed at about 650 °C for 18 h in the chamber, subsequently flashed at 1250 °C for 15 s by direct current heating while keeping the vacuum better than 1×10^{-9} mbar. Then, the substrate was cooled to about 900 °C at a rate of 2 °C/s. Finally, the clean Si(111)-(7×7) substrate was obtained and confirmed by STM images, as well as by low-energy electron-diffraction patterns.

An evaporation method with integral flux monitor (EFM) was used for Ge deposition. In the EFM evaporation, the bombarding electron beam induces a temperature rise of the Ge source (99.9999% purity) and causes its evaporation. The EFM can precisely control the deposition of fractions of monolayers up to multilayers. The typical growth rate was 0.01–0.02 ML/min ($1\ \text{ML}=7.8\times10^{14}$ atoms/cm^2), which was calibrated with Auger electron spectroscopy and flux. The temperature was checked by an optical pyrometer. During the deposition process, the substrate was kept at 150 °C. All the morphologies were investigated by STM at room temperature. Tips made by chemically etched tungsten wire with diameter of 0.13 mm and carefully cleaned in the UHV chamber were used for STM scanning.

For the first-principles quantum-mechanical calculations, the Si(111)-(7×7) surface was modeled by repeated slabs with four layers of Si atoms (188 Si atoms) and 12 Si adatoms, separated by a vacuum region of 12 Å. The geometry

 ©2007 The American Physical Society

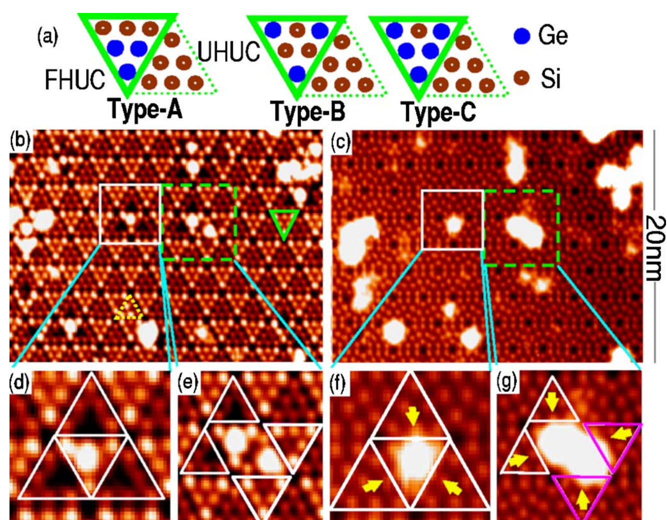

FIG. 1. (Color online) (a) Schematics for the three correlated patterns formed by single Ge atoms adsorbed on Si(111)-(7×7) for Ge coverages smaller than 0.1 ML. (b) Filled-state and (c) empty-state STM images of Si(111)-(7×7) after Ge deposition (0.12 ML). The solid and dashed triangles show the Ge triangular structure in a FHUC and a rare pattern containing individual Ge atoms in an UHUC, respectively. [(d)–(g)] Close-up images for the two characteristic patterns and the nearby areas in (b) and (c). The Si adatoms that are invisible in (d) and (e) are indicated by the arrows in (f) and (g).

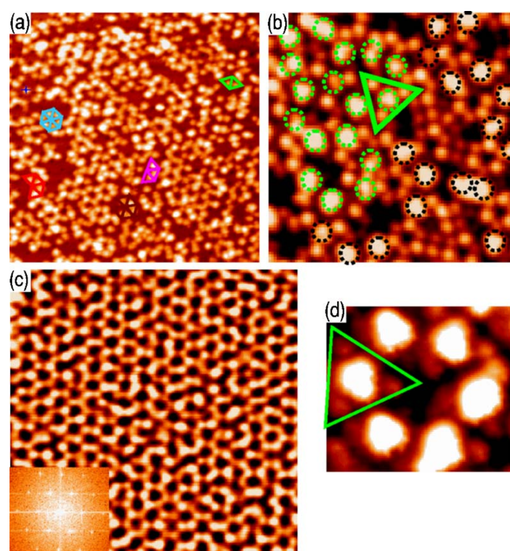

FIG. 2. (Color online) STM images of Ge/Si(111) at different Ge coverages. (a) 0.4 ML (V_s=+2.2 V, scanning area of 50×50 nm^2). Six distinct local nanostructures are indicated by different symbols. (b) 0.4 ML (V_s=−1.7 V, scanning area of 12×12 nm^2). The Ge nanoparticles in closed and open hexagonal rings are denoted by two different circles, respectively. (c) 0.5 ML (V_s=+2.6 V, scanning area of 50×50 nm^2). The inset image shows a Fourier transform of the hexagonal arrays. (d) 0.5 ML [filled-state image showing a closed hexagonal ring, corresponding to a local part in (c)]. The underlying triangular structure is indicated by a triangle in (b) and (d).

was adopted from the dimer-adatom-stacking fault (DAS) model.[16] The dangling bonds of the Si atoms at the bottom layer were terminated by hydrogen atoms. The numbers of Ge atoms in the Ge nanoparticles range from 3 to 12. All the Ge atoms are placed in the faulted half unit cell (FHUC). The adlayers and the top three Si layers were allowed to relax until the forces to the atoms were smaller than 0.05 eV/Å. An extensive search was made for the minimum-energy configurations of the Ge nanoparticles with various initial geometries. The calculations were performed within density-functional theory using the pseudopotential method and a plane-wave basis set.[17–19] A plane-wave energy cutoff of 150.6 eV and the Γ point in the irreducible part of the two-dimensional Brillouin zone of the 7×7 surface were used for relaxation calculations. However, the electronic density of states (DOS) was calculated with four special **k** points. The calculated DOSs for selected configurations with 14 special **k** points were found to be essentially the same as those obtained with four special **k** points.

III. RESULTS AND DISCUSSIONS

Our STM observations show that the evolution occurs in the following steps.

(i) At very low Ge coverages (smaller than 0.1 ML), most Ge atoms form correlated patterns replacing three or five out of the six so-called Si adatoms in the FHUC of the Si(111)-(7×7) reconstruction [Fig. 1(a)].[20]

(ii) At Ge coverages of ∼0.1–0.12 ML, a triangular lattice of single Ge atoms forms. The lattice is patterned by the FHUCs, which have a triangular shape. Ge atoms replace the Si adatoms at the corners of each FHUC [Fig. 1(b)], while only very few replacing the Si adatoms in unfaulted half unit cells (UHUCs).

(iii) When the Ge coverage is larger than ∼0.12 ML, Ge atoms begin to form isolated nanoparticles, mostly at the center of FHUCs, with typical diameters of 1.0 nm [Figs. 1(b)–1(d) and 1(f)], just fitting within FHUCs.

(iv) At larger local coverages, pairs of Ge nanoparticles appear in adjacent FHUCs and UHUCs [Figs. 1(b), 1(c), 1(e), and 1(g)]. The two nanoparticles are distinct, clearly separated by ∼6 Å. Gradually, complexes of three, four, and five Ge nanoparticles form, leading to complete hexagons (Fig. 2). Throughout the self-assembly of the hexagonal structures of nanoparticles, the underlying triangular lattice of single Ge atoms at the corners of only the FHUCs remains intact [Figs. 2(b) and 2(d)].

(v) Ordered arrays of hexagons superposed on the triangular lattice of single Ge atoms finally form at a coverage of ∼0.5 ML [Figs. 2(c) and 2(d)]. Since the resulting superstructure is templated by the underlying 7×7 surface, the net result is a three-level hierarchy of periodic structures. The structure does not show any changes over a temperature range of 27–470 K. At higher temperatures, however, the structure may become unstable. For example, a significant structural change was observed when the Ge nanostructure formed at room temperature with a coverage of ∼0.3 ML was annealed at a temperature of ∼573 K.[15]

In addition to the evolution of the hierarchical structure, the STM images reveal another feature that elucidates the driving mechanism. When an isolated Ge nanoparticle is formed in a FHUC, the electron density associated with center Si adatoms in the three surrounding UHUCs is depleted substantially, suggesting electron transfer to the Ge nanoparticle. As local coverage increases, when a new nanoparticle forms adjacent to an existing FHUC nanoparticle in a neighboring UHUC, electron transfer occurs from the two new surrounding FHUCs. The two nanoparticles remain distinct with a "dimer wall" separating them. First-principles calculations confirm the depletion of charge associated with the dangling bonds of center Si adatoms in the three UHUCs surrounding a Ge nanoparticle in a FHUC, and a decrease in electronic energy by such a charge transfer. The energy gain can be attributed to "local Madelung energy."

In Figs. 1(b)–1(g), we show contrasted filled-state (sample bias $V_s=-2.6$ V, tunneling current $I_t=0.2$ nA) and empty-state ($V_s=+2.6$ V, $I_t=0.2$ nA) STM images for the same region on Si(111)-(7×7) with a Ge coverage of 0.12 ML deposited at 150 °C. The identification of Ge atoms relative to Si atoms in the FHUCs was confirmed by profile lines which clearly show a distinct height difference of ~0.22 Å at the pertinent sites. While at low coverages, isolated adsorbed Ge atoms replace Si atoms in FHUCs and form the correlated patterns shown in Fig. 1(a),[16] a triangular lattice of isolated Ge atoms forms at about 0.12 ML. The Ge atoms occupy all the corner adatom sites of FHUCs [the type-B pattern in Fig. 1(a)]. Very few Ge patterns in UHUCs, such as that shown in Fig. 1(a) with a dotted triangle, are observed. At slightly higher local coverages, isolated Ge nanoparticles appear with a distinct preference for FHUCs. The Ge nanoparticles look more compact in the filled-state STM image than in the empty-state image [Figs. 1(b) and 1(c)]. The nanoparticles show strong brightness in the center region of the FHUCs. We estimated that a single-Ge nanoparticle contains approximately eight atoms. Note that the triangular single-atom structure underlying the Ge nanoparticles in the FHUCs remains intact with the formation of Ge nanoparticles.

A Ge nanoparticle in a FHUC has a strong effect on its three neighboring UHUCs. The closest Si center adatoms in the nearest-neighbor UHUCs are invisible in the filled-state STM image [Fig. 1(d)]. However, these Si adatoms remain at their original places in the 7×7 reconstruction, as shown by the empty-state STM image [Fig. 1(f)]. This fact suggests that the Si center adatoms transfer charge to the nearby Ge nanoparticle. The charge transfer is visible both in the filled-state STM images as darkened areas surrounding the nanoparticles, indicating absence of electrons and giving the nanoparticles a compact appearance with sharp outline, and in the empty-state STM images as extended brightness, making the nanoparticles appear less compact and blurring their outlines. Thus, the STM measurements demonstrate a lateral charge redistribution in the Ge-Si system. First-principles density-functional calculations for nanoparticles of 6–12 Ge atoms in the FHUC of a Si(111)-(7×7) unit cell show that, for all the minimum-energy configurations, the dangling-bond state of the center Si adatom that is near the FHUC is almost empty, indicating charge transfer. Figure 3(a) shows the projected electronic density of states (local DOS) onto the center Si adatom in an adjacent UHUC before and after the formation of a nine-Ge nanoparticle [Fig. 3(b)] in a FHUC. For the clean Si(111)-(7×7) surface (before Ge deposition), the dangling-bond state of the center Si adatom is partially occupied and crosses the Fermi level.[21–24] After the formation of the Ge nanoparticle, the occupation of the dangling-bond state is reduced significantly, confirming a charge transfer from the central Si adatom. Such a charge transfer occurs because it lowers the total energy of the system. Self-assembled nanoparticles of various metals formed on Si(111)-(7×7), which have similar network as Ge nanoparticles, have been reported.[25–33] While several groups suggested that the interaction between the substrate and the metal nanoparticles may play a role for the self-organization,[25–27] other researchers have emphasized the interaction between the nanoparticles themselves.[34] Charge transfer and its role have not been reported before.

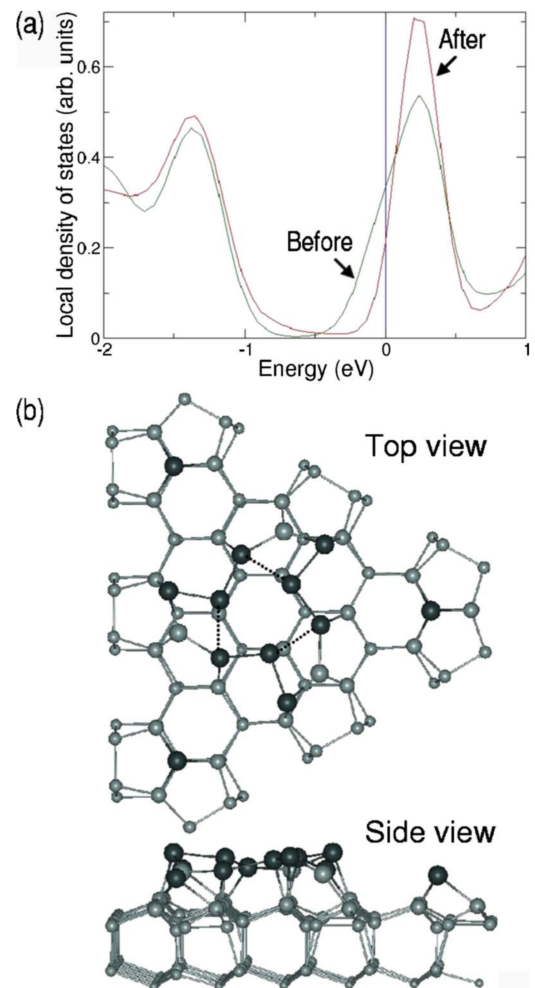

FIG. 3. (Color online) (a) Local density of states projected onto a center Si adatom in an UHUC before and after Ge deposition. The Fermi level is at 0 eV. (b) The corresponding relaxed minimum-energy configuration (only the FHUC is shown). The Si and Ge atoms are represented by gray and dark spheres, respectively. The Si atoms with increasing distances from the surface are shown by spheres of decreasing size. The dotted lines show weak bonds.

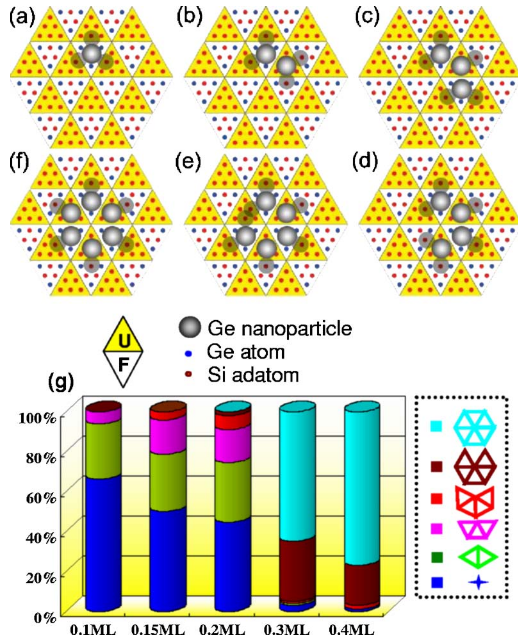

FIG. 4. (Color online) [(a)–(f)] Schematics illustrating the evolution and the three-level hierarchy of periodic structures. The Si center adatoms that transfer charge are shaded in gray. (g) Histograms for the distributions of different local Ge nanostructures at varying coverages.

When local coverage is higher, a second Ge nanoparticle may form at the center of an UHUC adjacent to a FHUC already containing a Ge nanoparticle, as shown in Figs. 1(e) and 1(g). Similar to the first one, the second Ge nanoparticle darkens the center Si atoms in the two neighboring FHUCs in the filled-state image [Fig. 1(e)], again indicating charge transfer, though the charge transfer is not as effective as in the UHUC. Charge transfer again helps us understand the formation of a nanoparticle in an UHUC when that UHUC is next to an existing particle in a FHUC. Assuming that the amount of charge transferred from any of the center Si adatom is the same (q_0), a single nanoparticle has a central charge of $-3q_0$ [Fig. 4(a)]. The total energy is lowered by a local Madelung energy, that is roughly $(-9/d_1+3/d_2)q_0^2$, where d_1 (~11 Å) is the distance between the Ge nanoparticle and an adjacent Si adatom that has been depleted of charge and d_2 (~19 Å) is the distance between two such Si adatoms. Because d_1 is smaller than d_2, the local Madelung energy is negative $(-0.66q_0^2)$. When a second nanoparticle forms in an adjacent UHUC, as in Fig. 4(b), the charge on each nanoparticle is reduced from $-3q_0$ to $-2q_0$ and the local Madelung energy is approximately $(-8/d_1+2/d_2+4/d_3)q_0^2 \approx -0.36q_0^2$, where d_3 (~15.5 Å) is the distance between the two Ge nanoparticles. The substantial reduction in the Madelung energy is used to overcome the factors that inhibit the formation of isolated nanoparticles in UHUCs and the residual Madelung energy stabilizes the pair (the energy is substantial; from the DOS curves of Fig. 3, we estimate $q_0 \approx (0.3-0.5)e$, whereby the Madelung energy that stabilizes a pair is ~0.5–1.3 eV).

Figures 2 and 4 show the continuing evolution of the nanoparticle superstructure into hexagonal patterns as the triangular lattice of single Ge atoms in corner adatom sites of FHUCs persists in the background. Starting with a pair in adjacent FHUC and UHUCs, the third Ge nanoparticle tends to form in one of the FHUCs near the first two, accompanied by charge transfer from the nearby Si adatoms in adjacent half unit cells. In this way, the fourth, fifth, and sixth nanoparticles gradually form, eventually resulting a hexagonal structure. Figures 2(a) and 2(b) show closed Ge hexagonal rings (with six nanoparticles), which begin to form at a Ge coverage of ~0.3 ML (not shown in the figure), and open rings (containing three, four, and five nanoparticles), nucleated on the Si(111) surface at a Ge coverage of ~0.4 ML. Figure 4(g) shows the distributions of different local nanostructures (isolated and pairs of Ge nanoparticles, open rings and closed hexagonal rings) at varying Ge coverages. When the Ge coverage approaches to ~0.4 ML, there are averagely ~20 Ge atoms per 7×7 unit cell. Thus, to accommodate the coverage of ~0.4 ML, most of the HUCs of both FHUC and UHUC types are occupied by Ge nanoparticles. We note that the net charge on each Ge nanoparticle decreases gradually from $3q_0$ in the case of an isolated nanoparticle to 2, 5/3, 3/2, 7/5, and finally $1q_0$ if a complete isolated hexagon were to form as in the schematic of Fig. 4. Thus, while the local Madelung energies contribute to the stabilization of the local structures, the effective Madelung energy per nanoparticle decreases as extended structures form and charging of the nanoparticle gradually fades as the ordered hexagonal structure is completed.

IV. SUMMARY

In summary, we show formation of a complex hierarchy of periodic structures: the underlying surface periodicity, a triangular structure of single Ge atoms, and a hexagonal structure of Ge nanoparticles. The evolution of the self-assembly of the Ge nanostructures on Si(111) has been tracked as a function of the amount of adsorbed Ge. The driving force for the self-assembly, that is, charge transfer and resultant "local Madelung energies," has been identified.

ACKNOWLEDGMENTS

We thank Y. L. Wang and H. M. Guo for their help. Access to the supercomputers at the National Center for Supercomputing Applications (under Grant No. DMR060010N) and at Oak Ridge National Laboratory is acknowledged. This work was supported in part by the national "973" and "863" projects, the Chinese Academy of Sciences, and by the William A. and Nancy F. McMinn Endowment at Vanderbilt University.

*Electronic address: hjgao@aphy.iphy.ac.cn
†Electronic address: sanwu-wang@utulsa.edu
‡Electronic address: pantelides@vanderbilt.edu

[1] A. P. Alivisatos, Science **271**, 933 (1996).
[2] F. Liu, F. Wu, and M. G. Lagally, Chem. Rev. (Washington, D.C.) **97**, 1045 (1997).
[3] K. Brunner, Rep. Prog. Phys. **65**, 27 (2002).
[4] C. Westphal, Surf. Sci. Rep. **50**, 1 (2003).
[5] J. Stangl, V. Holý, and G. Bauer, Rev. Mod. Phys. **76**, 725 (2004).
[6] H. Omi and T. Ogino, Phys. Rev. B **59**, 7521 (1999).
[7] F. Boscherini, G. Capellini, L. Di Gaspare, F. Rosei, N. Motta, and S. Mobilio, Appl. Phys. Lett. **76**, 682 (2000).
[8] Y. P. Zhang, L. Yan, S. J. Xie, S. J. Pang, and H. J. Gao, Appl. Phys. Lett. **79**, 3317 (2001).
[9] A. Lobo, S. Gokhale, and S. K. Kulkarni, Appl. Surf. Sci. **173**, 270 (2001).
[10] L. Yan, H. Q. Yang, H. J. Gao, S. S. Xie, and S. J. Pang, Surf. Sci. **498**, 83 (2002).
[11] F. Ratto, F. Rosei, A. Locatelli, S. Cherifi, S. Fontana, S. Heun, P. D. Szkutnik, A. Sgarlata, M. De Crescenzi, and N. Motta, Appl. Phys. Lett. **84**, 4526 (2004).
[12] H. M. Guo, Y. L. Wang, H. W. Liu, H. F. Ma, Z. H. Qin, and H. J. Gao, Surf. Sci. **561**, 227 (2004).
[13] Z. A. Ansari, T. Arai, and M. Tomitori, Surf. Sci. **574**, L17 (2005).
[14] F. Ratto, A. Locatelli, S. Fontana, S. Kharrazi, S. Ashtaputre, S. K. Kulkarni, S. Heun, and F. Rosei, Phys. Rev. Lett. **96**, 096103 (2006).
[15] Z. H. Qin, D. X. Shi, H. F. Ma, H.-J. Gao, A. S. Rao, S. Wang, and S. T. Pantelides, Phys. Rev. B **75**, 085313 (2007).
[16] K. Takayanagi, Y. Tanishiro, M. Takahashi, and S. Takahashi, J. Vac. Sci. Technol. A **3**, 1502 (1985).
[17] G. Kresse and J. Furthmüller, Comput. Mater. Sci. **6**, 15 (1996).
[18] J. P. Perdew, J. A. Chevary, S. H. Vosko, K. A. Jackson, M. R. Pederson, D. J. Singh, and C. Fiolhais, Phys. Rev. B **46**, 6671 (1992).
[19] D. Vanderbilt, Phys. Rev. B **41**, 7892 (1990).
[20] Y. L. Wang, H. J. Gao, H. M. Guo, S. Wang, and S. T. Pantelides, Phys. Rev. Lett. **94**, 106101 (2005).
[21] J. E. Northrup, Phys. Rev. Lett. **57**, 154 (1986).
[22] K. D. Brommer, M. Galvan, A. Dalpino, and J. D. Joannopoulos, Surf. Sci. **314**, 57 (1994).
[23] S. Wang, M. W. Radny, and P. V. Smith, J. Phys.: Condens. Matter **9**, 4535 (1997).
[24] S. Wang, M. W. Radny, and P. V. Smith, J. Chem. Phys. **114**, 436 (2001).
[25] L. Vitali, M. G. Ramsey, and F. P. Netzer, Phys. Rev. Lett. **83**, 316 (1999).
[26] J.-L. Li, J. F. Jia, X. J. Liang, X. Liu, J. Z. Wang, Q. K. Xue, Z. Q. Li, J. S. Tse, Z. Zhang, and S. B. Zhang, Phys. Rev. Lett. **88**, 066101 (2002).
[27] J. F. Jia, X. Liu, J. Z. Wang, J. L. Li, X. S. Wang, Q. K. Xue, Z. Q. Li, Z. Zhang, and S. B. Zhang, Phys. Rev. B **66**, 165412 (2002).
[28] K. Wu, Y. Fujikawa, T. Nagao, Y. Hasegawa, K. S. Nakayama, Q. K. Xue, E. G. Wang, T. Briere, V. Kumar, Y. Kawazoe, S. B. Zhang, and T. Sakurai, Phys. Rev. Lett. **91**, 126101 (2003).
[29] M. Y. Lai and Y. L. Wang, Phys. Rev. Lett. **81**, 164 (1998).
[30] M. Y. Lai and Y. L. Wang, Phys. Rev. B **64**, 241404(R) (2001).
[31] H. H. Chang, M. Y. Lai, J. H. Wei, C. M. Wei, and Y. L. Wang, Phys. Rev. Lett. **92**, 066103 (2004).
[32] M. A. K. Zilani, Y. Y. Sun, H. Xu, Y. P. Feng, X. S. Wang, and A. T. S. Wee, Phys. Rev. B **72**, 193402 (2005).
[33] M. A. K. Zilani, H. Xu, T. Liu, Y. Y. Sun, Y. P. Feng, X. S. Wang, and A. T. S. Wee, Phys. Rev. B **73**, 195415 (2006).
[34] E. Vasco, C. Polop, and E. Rodriguez-Canas, Phys. Rev. B **67**, 235412 (2003).